Brazilian Journal of Analytical Chemistry
Pre-publication – Accepted after peer review
doi: 10.30744/brjac.2179-3425.AR-22-2025

BrJAC

ARTICLE

Fabrication of an Electrochemically Synthesized Nanoporous Gold Electrode for *In-Situ* Ascorbic Acid Determination in Fruit Samples

Eduarda Soldi Sartori Seixas, Pedro Henrique Alves Damasceno, Gilberto José Silva Junior*, Mauro Bertotti

Departamento de Química Fundamental, Instituto de Química, Universidade de São Paulo
Av. Prof. Lineu Prestes, 748, 05508-000, São Paulo, SP, Brazil

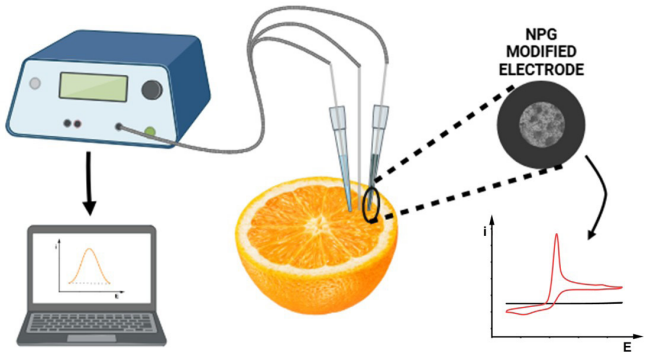

In this report, we present the development of a nanoporous gold (NPG) modified electrode fabricated through a mold-assisted electrodeposition technique, wherein a gold film was deposited onto a gold microfiber substrate. This modified electrode was subsequently employed for the *in-situ* determination of ascorbic acid (AA) in orange and lime juice samples. The NPG-modified electrode exhibited a high edge density, which contributes to an enhanced electrochemically active surface area, promoting a favorable electrocatalytic effect for the anodic oxidation of AA and resulting in a significantly lowered oxidation potential. Differential pulse voltammetry (DPV) measurements revealed a detection limit of 10 µmol L^{-1} and a quantification limit of 30 µmol L^{-1}. The NPG-modified electrode demonstrated outstanding analytical performance, displaying both high sensitivity and selectivity for AA determination in a complex matrix (orange and lime juice). The voltammetric data were corroborated with coulometric experiments, further validating the reliability of the electrochemical determination of AA using the NPG-modified electrode. Thus, this work highlights the potential of this novel electrochemical sensor, presenting a straightforward and efficient approach for NPG sensor fabrication, and underscoring its substantial promise for *in-situ* analytical applications.

Keywords: nanoporous gold electrode, *in-situ* analysis, ascorbic acid, electrocatalytic effect, food samples

INTRODUCTION

Fruits and vegetables are extensively recommended by health professionals for human consumption due to their rich nutritional profiles.[1] Beyond their nutritional value, these foods contain bioactive compounds that exhibit antioxidant properties, critical in mitigating oxidative stress and protecting against natural degenerative

Cite: Seixas, E. S. S.; Damasceno, P. H. A.; Silva Junior, G. J.; Bertotti, M. Fabrication of an Electrochemically Synthesized Nanoporous Gold Electrode for *In-Situ* Ascorbic Acid Determination in Fruit Samples. *Braz. J. Anal. Chem.* (Forthcoming). http://dx.doi.org/10.30744/brjac.2179-3425.AR-22-2025

Submitted April 3, 2025; Resubmitted July 11, 2025; Accepted August 18, 2025; Available online September 2025.

This article was submitted to the BrJAC special issue on the 21st ENQA and 9th CIAQA.

processes associated with premature aging and different diseases. Among the primary phytochemicals recognized for their antioxidant properties is vitamin C, also known as ascorbic acid (AA).[2,3]

AA is an antioxidant and water-soluble vitamin. Under certain physiological conditions, it also exists in its anionic form (ascorbate), which has a hexanoic sugar acid structure and contains two dissociable protons with pKa values of 4.04 and 11.34.[4] In addition to its antioxidant properties, AA facilitates the collagen synthesis, a critical component for maintaining healthy cartilage, skin, and bone tissue. Furthermore, it modulates cytokine production, enhances the rate of wound healing, and increases the synthesis of antibodies within the organism, among other physiological functions.[5,6]

In this context, the daily intake of foods rich in ascorbic acid is essential for maintaining bodily health. Among the fruits that serve as sources of ascorbic acid, certain varieties are particularly prominent for their high content, such as Barbados cherry, strawberry, lemon, and orange.[7] This study will specifically focus on determining AA in orange samples, as oranges are among the foods with the highest concentrations of vitamin C and are commonly consumed in daily diets. Factors such as climate, harvesting method, storage, and processing of fruits can cause variability in the AA content in foods.[8] In this regard, a rapid, simple, and effective method for determining vitamin C in food samples with high sensitivity and selectivity is highly desirable.

Different analytical techniques have been reported for detecting AA in various food samples. Among the more traditional instrumental methods, the literature highlights AA determination via fluorescence,[9,10] capillary electrophoresis coupled to mass spectroscopy,[11] high-performance liquid chromatography coupled to a colorimetric device[12] or to an UV-VIs detector,[13] etc. While these techniques offer high sensitivity for AA detection, they necessitate sophisticated, bulky, and expensive instrumentation, often associated with prolonged analysis times and the consumption of reagents. In this context, the development of electrochemical sensors for AA detection becomes highly advantageous, given their cost-effectiveness, miniaturization, and exceptional sensitivity and selectivity.

To enhance the sensitivity and selectivity of analytical determinations, the modification of electrode surfaces with materials possessing high surface area represents a straightforward and effective strategy. For instance, various nanomaterials have been prepared using different approaches and extensively used for several applications.[14-17] Among the various nanomaterials, NPG has gained prominence in the field due to its advantageous properties, such as excellent chemical stability, high surface area, outstanding electrical conductivity, and catalytic properties, which can enhance the determination of AA in fruit samples.[18]

Recent studies have focused on the fabrication of NPG-modified electrodes using approaches such as dealloying gold-containing alloys,[19,20] anodic corrosion of gold surfaces,[21] and synthesizing of hybrid films containing gold nanoporous and carbon-based materials for different applications.[22] Kumar and colleagues further reported their efforts in developing an NPG-modified electrode via mold-assisted electrodeposition to determine AA in biological samples.[23] However, it is noteworthy that, to date, no efforts have been reported on the fabrication of NPG-modified electrodes via electrodeposition for in-situ analysis in orange juice.

Paixão et al.[24] previously reported the use of a lab-made platinum microelectrode for mapping ascorbic acid in oranges. Their study focused on potential concentration differences of ascorbic acid across various fruit regions. In contrast, our research is centered on the development of a sensitive platform that facilitates the anodic oxidation of ascorbic acid, leveraging the physicochemical properties of nanoporous gold films. In this context, we present a rapid amperometric strategy for fabricating an NPG film on a lab-made gold microsensor surface for the determination of AA in natural orange juice samples. NPG-modified electrodes were fabricated using the Dynamic Hydrogen Bubble Template (DHBT) method,[25] and to optimize the platform, a comprehensive study was conducted by adjusting the experimental electrodeposition parameters to prepare NPG films under ideal conditions. In addition to the aforementioned advantages, the electrode developed in this work also presents a low fabrication cost, estimated at approximately USD 4.00 per device, which qualifies it as a low-cost analytical platform.

Notably, the electrochemical data obtained from the new amperometric microsensor based on NPG were found to be in excellent agreement with coulometric measurements in the same samples, thus validating the effectiveness and reliability of this novel approach.

MATERIALS AND METHODS

Chemicals

$HAuCl_4 \cdot 3H_2O$, ascorbic acid (AA), citric acid, folic acid, and glutamic acid were acquired from Sigma-Aldrich (St. Louis, MI, USA). Acetic acid, sodium acetate, potassium iodide, sodium sulfate, potassium chloride, D-(+)-glucose, and sulfuric acid (H_2SO_4) were purchased from Merck (Darmstadt, Germany), and soluble starch from Reagen (Paraná, Brazil). All the reagents were analytical grade and used without further purification unless otherwise stated. The solutions were prepared using Milli-Q water with 18 MΩ cm resistivity.

Experimental apparatus

Electrochemical measurements were conducted using an Autolab PGSTAT128N potentiostat interfaced with NOVA 2.0 software. The experiments were performed in a three-electrode configuration, employing a gold microelectrode, Ag/AgCl (saturated KCl), and a platinum wire as the working, reference, and counter electrodes, respectively. The gold electrode was polished with alumina powder (0.05 µm), rinsed with large quantities of distilled water, and subjected to ultrasonic cleaning for several seconds. Subsequently, the electrochemical behavior was assessed in a 0.5 mol L^{-1} H_2SO_4 solution, and the cleaning procedure was repeated until a reproducible gold electrochemical response was achieved. Surface morphology images of nanoporous gold were acquired using field emission-scanning electron microscopy (FE-SEM) with a JOEL JSM-7401F (30 kV) instrument. The coulometric system consists of a cell with a platinum net (anode) immersed in 50 mL of acetate buffer (pH 4.0) with 2 g of KI, 1 mL of a starch indicator, and 0.5 mL of the sample. Another platinum electrode kept inside a protection tube filled with a 0.5 mol L^{-1} Na_2SO_4 solution was used as a cathode. The protection tube was in contact with the rest of the cell through a membrane, and the starch indicator was prepared by adding 1 g of soluble starch in 100 mL of boiling distilled water.

Fabrication of bare Au and NPG-modified electrodes

The bare gold microelectrode was prepared from a gold fiber (99.99%, 0.025 mm, GoodFellow®) sealed in the tip of a micropipette using Araldite® epoxy glue. The interior of the pipette tip was filled with carbon black to ensure electrical contact and a nickel-chromium wire was inserted. The pipette tip was sealed with Parafilm paper. The fabricated electrode was polished using 600-grit sandpaper to remove excess glue, followed by 1200-grit sandpaper to expose the gold fiber.

The electrodic surface modification step was carried out using a mold-assisted electrodeposition approach known as DHBT. The microelectrode prepared in the previous step was immersed in a 5.0 mmol L^{-1} $HAuCl_4$ solution in 0.5 mol L^{-1} H_2SO_4, and using an amperometric approach, a potential of -3 V was applied during 100 s, forming a highly porous structure, the NPG-modified electrode. The potential and deposition time values were properly optimized. After each step, the electrochemical characterization was performed by cyclic voltammetry (CV) in a 0.5 mol L^{-1} H_2SO_4 solution.

Analytical parameters for AA determination

The analytical curve was obtained in a 30 to 100 µmol L^{-1} AA concentration range in acetate buffer (pH 4.0) using the DPV technique. Acetate buffer in this pH was chosen because such a value is close to the one found in natural orange juice (pH around 4.2). The AA anodic response was recorded in the potential range from -0.2 to 0.6 V (vs. Ag/AgCl sat. KCl), and the optimized parameters were determined as pulse amplitude 50 mV, step potential 5 mV, and scan rate 50 mV s^{-1}. Measurements were performed in triplicate for each concentration to estimate the precision.

The AA concentration in natural orange juice and in natural lime juice was determined using the standard addition method where 60 µL of a 0.1 mol L^{-1} AA in acetate buffer (pH 4.0) solution was added five times to the juice. After each addition, measurements were done using DPV, and three replicates were performed to estimate the precision. Coulometry titration was employed as a validation method using a constant current of 0.01 A.[26]

Pretreatment of natural orange juice and natural lime juice samples

The oranges and limes employed in these experiments were from the *Citrus sinensis* and *Citrus latifolia* species, respectively. The samples were prepared by squeezing the fruits separately and filtering the juice using qualitative filter paper. The analyses were conducted on the same day the samples were prepared.

RESULTS AND DISCUSSION

Morphological characterization

The both bare and NPG-modified electrodes' structural morphology study was performed using Field Emission Scanning Electron Microscopy (FE-SEM) images (Figure 1). A gold microfiber was immersed halfway into a 5.0 mmol L^{-1} $HAuCl_4$ in 0.5 mol L^{-1} H_2SO_4 solution to obtain the NPG film, enabling a clear comparison between the bare and modified microfiber regions (Figures 1A, 1E). Amplified images of both areas (Figures 1B, 1F) highlight their differences. The bare gold microfiber (Figures 1A, 1B) shows a smooth surface, with only a few tiny traces inherent to the commercial microfiber. The NPG-modified microfiber, obtained on the day of image acquisition, displays a porous film over the fiber, showing increased surface area and roughness with nanoporous structures (Figures 1E, 1F).

SEM images of the bare and NPG-modified electrodes surfaces were also obtained (Figures 1C, 1D, 1G, 1H). The bare electrode images (Figures 1C, 1D) show the shape of a cross-sectional area of the microfiber. The amplified image (Figure 1D) reveals a smooth surface without significant roughness. In contrast, the SEM images of the NPG-modified electrode (Figures 1G, 1H) show the nanostructures obtained. The SEM images of the NPG-modified electrode surface were obtained on an electrode modified ten days before the images were taken. Even after ten days, the NPG morphology remains, demonstrating mechanical stability. The amplified image of the NPG-modified electrode (Figure 1H) also shows the nanometer-sized pores obtained.

In all NPG images, the honeycomb-like formation of the NPG film on the material's surface is visible. This formation leads to an increase in the surface area due to the gold deposition assisted by the hydrogen bubbles formed and an increase in roughness, as seen in the formation of the porous structure.[18,27-29]

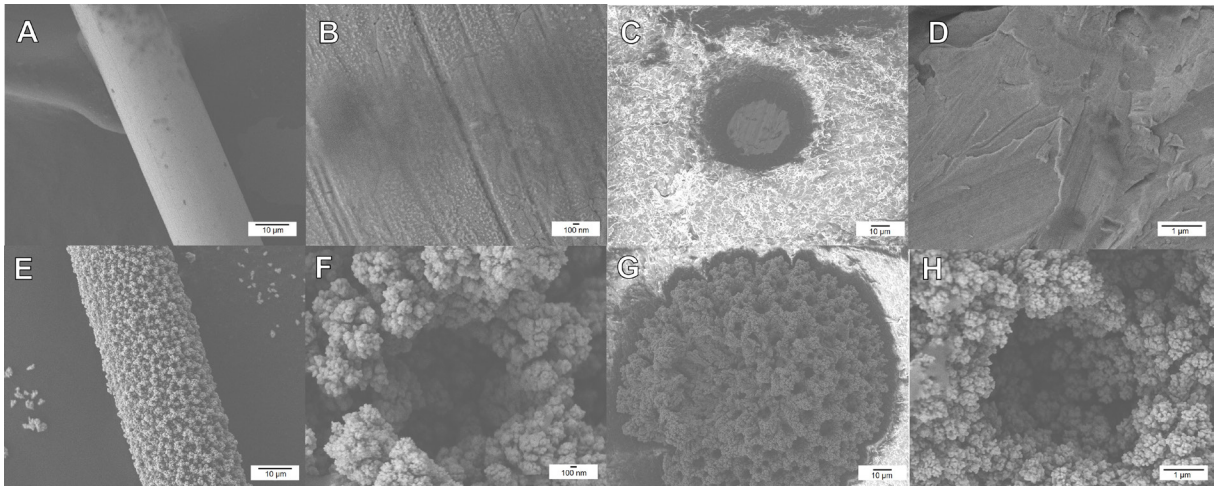

Figure 1. SEM images of a bare gold microfiber 1400X magnified (A) and 30000X magnified (B), a gold bare microelectrode 750X magnified (C) and 16000X magnified (D), a modified microfiber with NPG 1400X magnified (E) and 30000X magnified (F), an NPG-modified electrode 750X magnified (G) and 16000X magnified (H).

Electrochemical characterization

The electrochemical characterization was carried out by CV using the bare and NPG-modified electrodes in a 0.5 mol L^{-1} H_2SO_4 solution, and the results are shown in Figure 2. As one can see, distinct voltammetric

profiles were obtained for the bare and the NPG-modified electrodes. A single anodic current peak was observed at E = 1.4 V for the bare microelectrode. In contrast, the voltammogram for the NPG-modified electrode shows two anodic peaks at E = 1.2 V and E = 1.4 V. The difference between the profiles obtained on the different surfaces and the two oxidation peaks on the NPG-modified electrode are attributed to the formation of new crystalline planes of the deposited gold during the electrode surface modification.[27]

During the reverse scan, a remarkable cathodic current peak (E = 0.9 V) is noticed for the NPG-modified electrode. Hence, the electrochemically active surface area (ECSA) was determined according to the Equations 1 and 2:[25]

$$Charge\ (C) = \frac{Cathodic\ peak\ area}{Scan\ rate\ (Vs^{-1})} \quad (1) \qquad ECSA\ (cm^{-2}) = \frac{Charge}{390\ \mu C\ cm^{-2}} \quad (2)$$

The modified electrode ECSA increased about 1500-fold when compared to the bare electrode. This area increase is attributed to changes in surface morphology promoted by the gold electrodeposition, as shown in the SEM images of the surface (Figure 1).

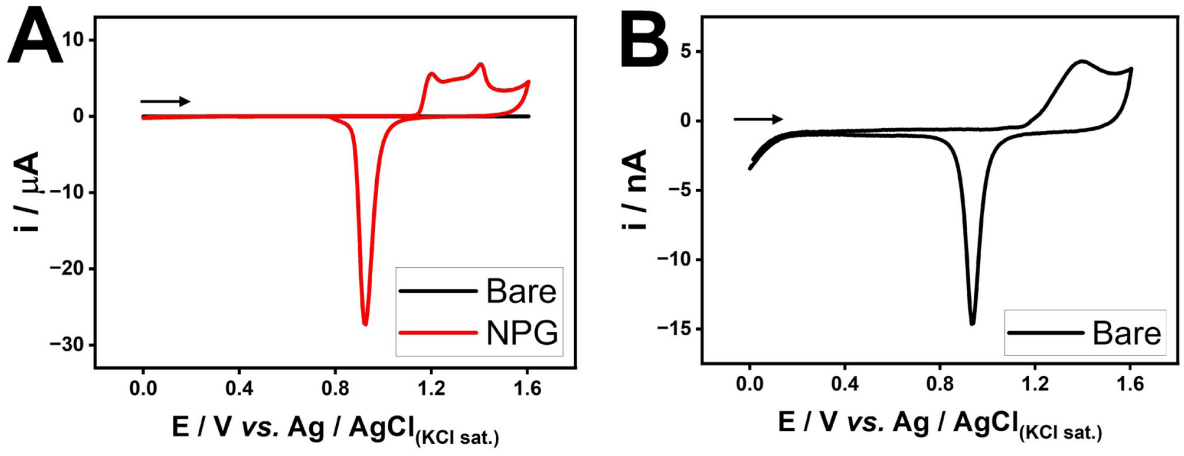

Figure 2. CVs of bare (black curve) and NPG-modified (red curve) electrodes recorded in a 0.5 mol L^{-1} H_2SO_4 solution (A) and magnified CV of the bare microelectrode (B). (Scan rate:100 mV s^{-1}).

Electrochemical behavior of ascorbic acid (AA)

AA undergoes oxidation to dehydroascorbic acid (DA) through a two-electron electrochemical reaction.[4,25,29]

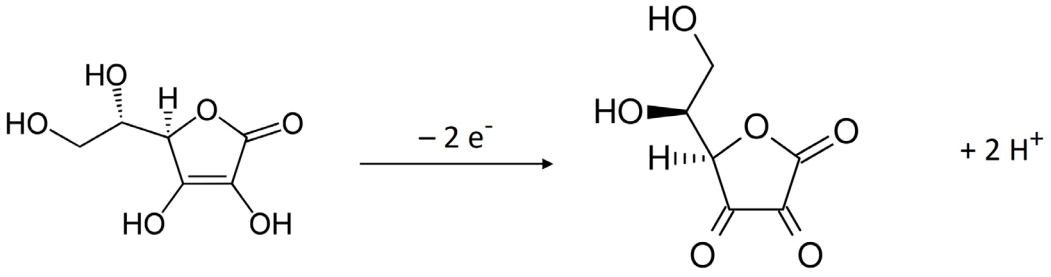

Equation 1

The electrochemical behavior of AA was investigated by CV in a potential window from 0.6 to -0.2 V in a 3.0 mmol L^{-1} AA solution in acetate buffer (pH 4.0) and the obtained CVs for both bare and NPG-modified electrodes are shown in Figure 3. The voltammetric profile obtained using the bare microelectrode

(Figure 3B) clearly demonstrates the anodic current generated during the oxidation of ascorbic acid in comparison to the background signal.

Figure 3A shows the comparative study of the electrochemical behavior of AA using both bare and NPG-modified electrodes. The CV recorded with the NPG-modified electrode (red curve) presented a maximum current that is 42-fold higher than the bare Au electrode and a clear anticipation of the onset potential. The observed increase in anodic current can be attributed to the significant enhancement of the ECSA. The NPG film allows AA to penetrate the pores; hence, a larger area is available for the electrochemical reaction, and a pre-concentration occurs within the pores, as evidenced by the first cycle of CV. In subsequent cycles, a slight decrease in anodic current is observed due to the fast electron transfer, leading to the oxidation of AA to DA without significant diffusion through the NPG film (Figure 1S).

The potential shift associated with the anodic process toward less positive values can be explained by the formation of new crystalline planes in the deposited gold film.[27, 28] These new surfaces allow different mechanisms associated with the AA oxidation, resulting in a more facile electron transfer process.[25,27] Additionally, the species nanoconfinement in the pores increases the probability of the reaction occurrence, as the species are close to the electrode surface. The NPG film also enables better coordination between the electroactive species and the gold atoms, especially at the edges of the structures, facilitating better contact between the species and the electrode surface. Finally, the nanostructured defects enhanced the synergy between AA and the electrode surface.[27,28]

The AA anodic oxidation at the NPG-modified electrode presents a sharp peak at around 0.15 V (Figure 3A). This voltammetric shape reflects the fast electron transfer occurring at the NPG surface, and because AA is rapidly oxidized to DA, such electroactive species is rapidly depleted and generates a peak that is unusual for a microelectrode at conventional scan rates. Such behavior also reveals that AA in the bulk of the solution takes longer to penetrate the pores.

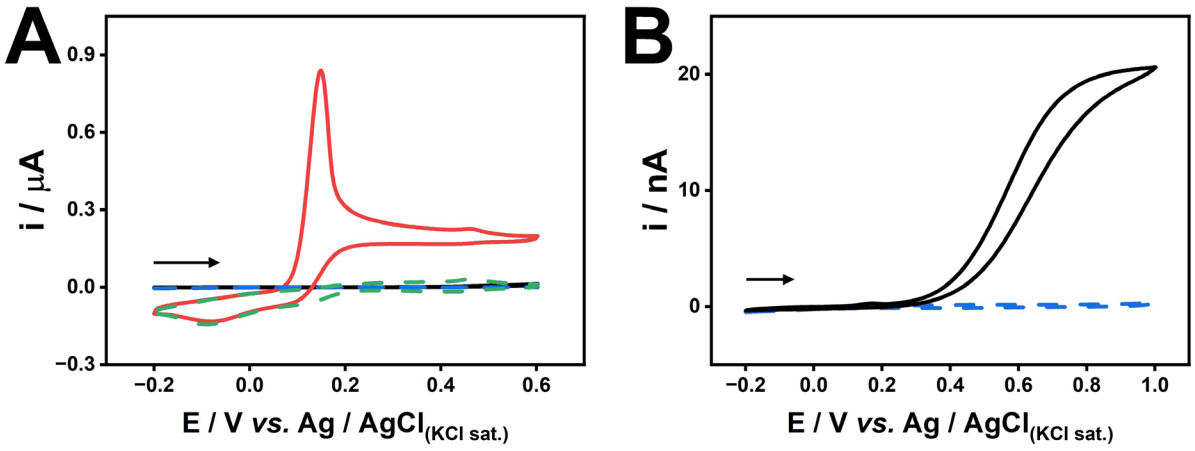

Figure 3. CVs recorded in a 3.0 mmol L^{-1} AA solution in acetate buffer (pH 4.0) using bare (black curve) and NPG-modified (red curve) electrodes (A) and CVs recorded in acetate buffer (pH 4.0) solution using bare (blue curve) and NPG-modified (green curve) electrodes (A). Magnified CVs recorded using the bare electrode (B). (Scan rate: 100 mV s^{-1}).

Analytical performance

Analytical parameters

To determine the limit of detection (LOD) and the limit of quantification (LOQ), calculated according to the IUPAC recommendations,[30] an analytical curve between 30 and 100 µmol L^{-1} was recorded in acetate buffer (pH 4.0) using the NPG-modified electrode (Figure 2S). A correlation coefficient of 0.9933 was found, the LOD was determined as 10 µmol L^{-1}, and the LOQ was determined as 30 µmol L^{-1}.

A comparison of key analytical parameters between the sensor developed in this work and other electrochemical sensor reported in the literature is presented in Table I. Compared to previously reported methods, the strategy developed in this work achieves a low limit of detection, which are either superior or comparable to those reported for other electrochemical sensors. Importantly, this level of sensitivity is achieved through a simple electrochemical deposition process completed in only 100 seconds. In contrast, many existing approaches rely on multi-step fabrication procedures, including nanomaterial synthesis, thermal treatment, or sequential deposition steps, all of which increase the complexity, cost, and duration of electrode preparation.

The sensor developed herein is based on a direct electrochemical modification using low-cost and commercially available materials, without requiring additional chemical synthesis, drop-casting, or sophisticated instrumentation. The linear concentration range obtained, along with the low detection limit, is fully suitable for the determination of the target analyte in fruit juice samples. These features highlight the practical applicability of the proposed sensor and support its potential as a reliable and efficient platform for routine electrochemical analyses.

Table I. Comparison of different modified electrodes and electroanalytical techniques for AA

Surface	Technique	Linear range μmol L^{-1}	LOD μmol L^{-1}	Sample	Ref.
PdNPs/rGO/GCE	DPV	300 – 30000	100	Human serum	31
NPG	DPV	320 – 3400	63	FBS	32
e-NCNF	AMP	50 – 1000	20	Rat brain microdialysates	33
ITO-rGO-AuNPs	LSV	20 – 150	9.4	Milk, fruit juice, urine	34
AuNPs/PAN	AMP	10 – 1000	8.8	–	35
erGO/TiS_2//GCE	AMP	0.1 – 1	0.03	Vit C tablets	36
ITO/gC_3N_4/NC@GC/h-ATS	DPV	0.05 – 200	0.02	Urine	37
NPG	DPV	30 – 100	10	Fruit juice	This work

Interference study

A study was performed to understand the response of AA in the presence of possible interferents commonly found in orange juices, including folic acid (FA), glutamic acid (GA), citric acid (CA), and glucose (GLU). Experiments were performed by fixing the AA concentration at 1 mmol L^{-1} and adding the other compounds in the same proportion they can be found in orange juices (1:0.003 for AA:FA, 1:0.6 for AA:GA, 1:10 for AA:CA, and 1:30 for AA:GLU).[38] Based on the results presented in Figure 4, it can be concluded that none of the tested species significantly influenced the AA quantification, with interference remaining at 5% for GA, 7% for GLU, and no interference was observed for the other species studied. One can conclude that the synergistic effect of the NPG film on the electron transfer rate involved in the AA anodic oxidation makes the proposed sensor highly selective for determining this analyte in orange samples.

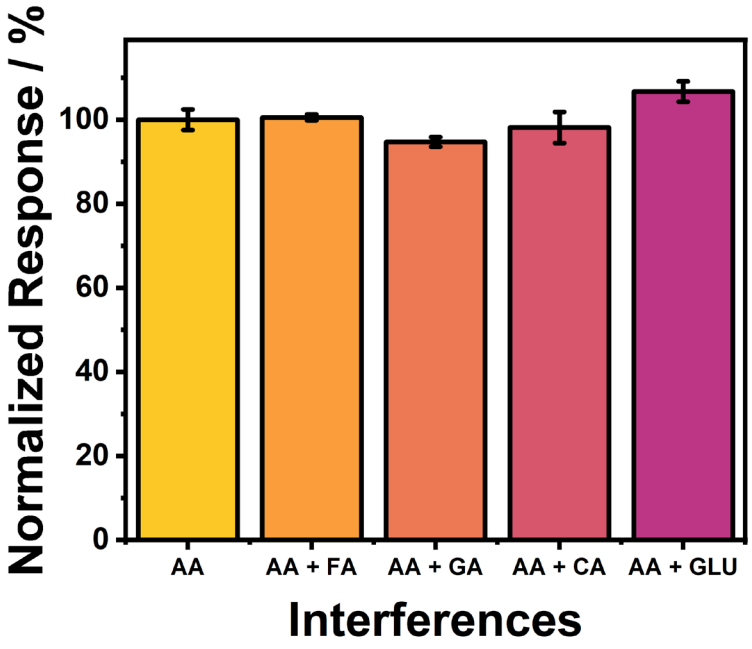

Figure 4. Interference study performed in solutions containing 1.0 mmol L^{-1} AA in the absence and presence of the possible interfering species: folic acid (FA), glutamic acid (GA), citric acid (CA), and glucose (GLU) using the NPG electrode.

Real samples

The developed NPG-modified electrode was applied to quantify AA in a natural orange juice sample. Due to a matrix effect, which can be caused by the presence of interferences such as GA and GLU, along with the differences in viscosity and conductivity, the AA signal obtained in the juice and by inserting the electrode into the fruit differed from that obtained in buffer solutions, as shown in Figure 5. Therefore, the juice's background signal was obtained by adding slices of *Cucumis sativus*, a species of cucumber known for its two peroxidases that degrade AA,[39] to a previously separated sample of the juice and leaving it in agitation for five hours.

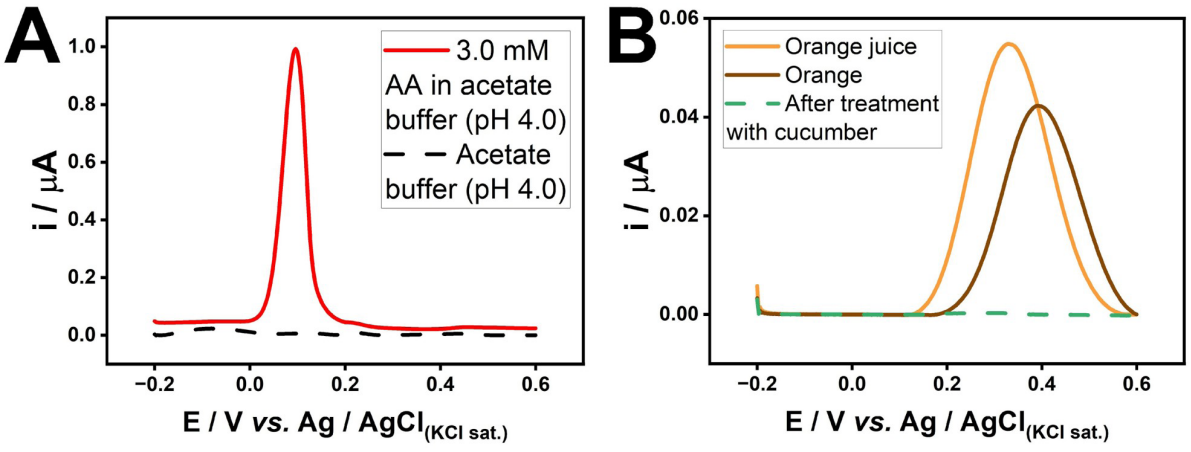

Figure 5. DPVs recorded in 3.0 mmol L^{-1} AA solution in acetate buffer (pH 4.0) and acetate buffer (pH 4.0) solution (A) and in natural orange juice, directly in an orange and after treatment with cucumber (B), using NPG-modified gold electrodes.

Due to this difference, the AA determination was carried out using the standard addition method, as shown in Figure 6. The results were compared to those obtained through coulometry, a comparative method for AA determination[26] performed on the same sample (Table II).

Table II. AA concentration determined in natural orange juice using DPV and coulometry

Method	AA Concentration mmol L^{-1}	RSD %
DPV	1.7 ± 0.1	5.9
Coulometry	1.6 ± 0.1	6.2

The proposed sensor's attractive features (selectivity and small size) made it possible to record the AA response directly in an orange (the same one used to prepare the orange juice, CV shown in Figure 5B, brown curve). The obtained signal was compared to the background corrected standard addition curve, shown in Figure 6C, and the concentration found in the orange was 1.1 ± 0.2 mmol L^{-1}.

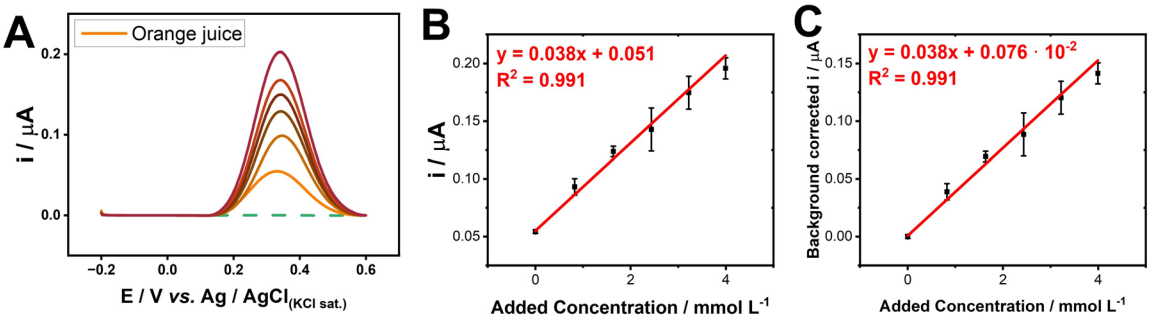

Figure 6. DPVs recorded in natural orange juice before and after additions of a standard 100 mmol L^{-1} AA solution in acetate buffer (pH 4.0) (A). Standard addition curve (B) and background corrected standard addition curve (C).

The developed sensor was also applied to quantify AA in natural lime juice by following the same steps used to quantify AA in natural orange juice. The standard addition curve is presented in Figures 7A and 7B, and the background-corrected standard addition curve is shown in Figure 7D. Results were compared to those obtained through coulometry for the same sample and are shown in Table III. The response was also recorded directly in the lime (Figure 7C), and the concentration was found to be 2.1 ± 0.1 mmol L^{-1}.

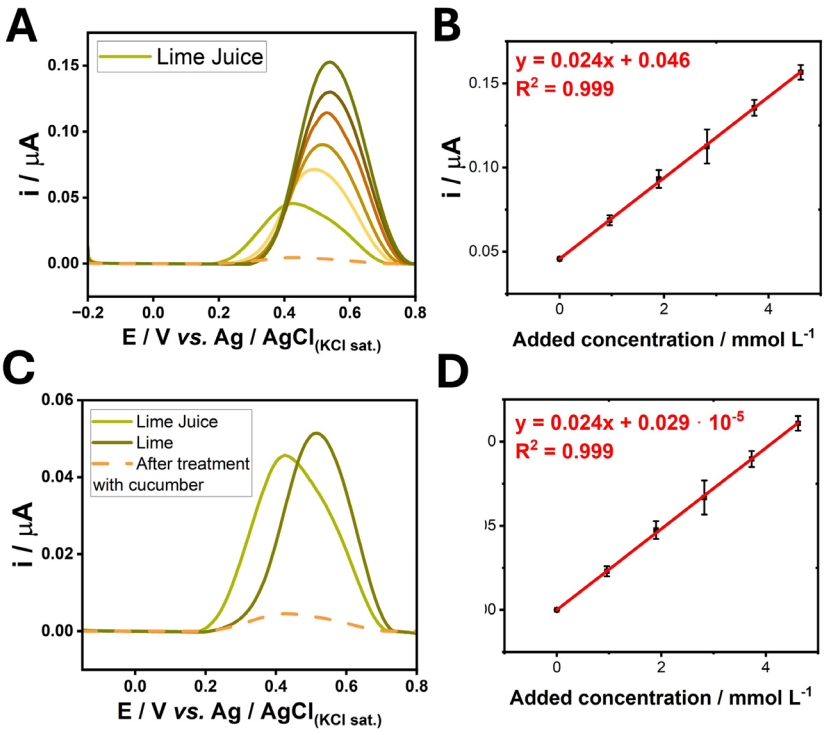

Figure 7. DPVs recorded in natural lime juice before and after additions of a standard 100 mmol L^{-1} AA solution in acetate buffer (pH 4.0) (A). Standard addition curve (B). DPVs recorded in natural lime juice, directly in the lime and after treating the natural juice with cucumber (C). Background corrected standard addition curve (D).

Table III. AA concentration determined in natural lime juice using DPV and coulometry

Method	AA Concentration mmol L^{-1}	RSD %
DPV	1.9 ± 0.2	10.5
Coulometry	1.5 ± 0.2	13.3

Coulometry titration can be a fast analysis but, as mentioned in the *Experimental apparatus* section of this article, besides having a visual end point that can be susceptible to human error, its system requires the use of 1 mL of starch indicator, 2 g of KI, and 50 mL of acetate buffer for this kind of analysis. Coulometry is known for the capability of sequential analysis using the same cell. However, since natural juices are colorful, it was necessary to prepare a new cell for each measurement in order to maintain the same endpoint, which significantly increased the reagent waste. Our study also showed that in cases of natural orange juice and in natural lime juice, coulometry RSD was higher.

The response stability of the NPG-modified electrode was also examined. If manipulated and stored under proper conditions, i.e., without physical impacts on the surface, stored in a 0.5 mmol L^{-1} H_2SO_4 solution, and electrochemically cleaned before and after each day of use (by recording 100 cycles of CV with a 500 mV s^{-1} scan rate in a 0.5 mol L^{-1} H_2SO_4 solution), the response can last about a month without significant loss, presenting less than 10% decrease after 25 days. After this time, the NPG-modified electrode no longer presents an ideal electrochemical behavior. Stability study results are presented in the supplementary material (Figure 3S). Results of a memory effect study, where sequential voltammograms recorded in

a solution without AA after keeping the electrode in solution containing AA, were also performed, and negligible signals can be noticed (Figure 4S). This confirms the absence of memory effects.

CONCLUSIONS

We have reported a novel approach to using NPG-modified electrodes, whose surface was modified by a rapid amperometric strategy, for detection and quantification using differential pulse voltammetry of AA in natural orange juice, natural lime juice, and for *in situ* analysis within an orange and a lime. The fast protocol of modifying the electrode surface significantly enhances the sensor's sensitivity and selectivity toward AA detection due to an electrocatalytic effect promoted by the nanoporous structure. We also demonstrated that the NPG-based electrode retains its electrochemical performance and structural integrity even when applied directly within fresh fruit tissue (a slightly rigid and heterogeneous matrix) without any pre-treatment or sample preparation. Further studies are of interest to better understand the matrix effect responsible for a significant change in the AA response in such a sample. The results showed that the obtained LOD is way lower than the AA concentration found in the fruits and the juices, justifying the use of the NPG-modified electrode for this approach. The proposed sensor yielded reliable results regarding the AA content in oranges and limes, besides being simple, cheaper, wasting fewer reagents, and not requiring sophisticated, bulky, and expensive instrumentation. Finally, we also reported the proper conditions for manipulating and storing the NPG-modified electrode, giving the modification a long service life.

Conflicts of interest

The authors declare that there are no known competing financial interests or personal relationships that could have appeared to influence the work reported in this paper.

Acknowledgements

The authors would like to thank the financial support from the São Paulo State Research Foundation, FAPESP [Grant numbers 2023/00246-1, 2022/03643-9, 2025/00748-2], and the National Council for Scientific and Technological Development, CNPq [Grant Number: 103418/2024-5].

REFERENCES

(1) Kitts, D. D. An evaluation of the multiple effects of the antioxidant vitamins. *Trends Food Sci. Technol.* **1997**, *8* (6), 198-203. https://doi.org/10.1016/S0924-2244(97)01033-9

(2) Aishwarya, K. D.; Nayaka, Y. A.; Pradeepa, E.; Sahana, H. R. Electrochemical determination of ascorbic acid using sensitive and disposable methylene blue modified pencil graphite electrode. *Anal. Biochem.* **2025**, *698*, 115733. https://doi.org/10.1016/j.ab.2024.115733

(3) Yaacob, S. F. F. S.; Din, S. N. M.; Suah, F. B. M. Ascorbic acid sensor using modified pencil graphite electrodes: a preliminary study. *Russ. J. Electrochem*. **2024**, *60*, 392-399. https://doi.org/10.1134/s1023193524050094

(4) Pisoschi, A. M.; Pop, A.; Serban, A. I.; Fafaneata, C. Electrochemical methods for ascorbic acid determination. *Electrochim. Acta* **2014**, *121*, 443–460. https://doi.org/10.1016/j.electacta.2013.12.127

(5) Tajima, S.; Pinnell, S. R. Ascorbic acid preferentially enhances type I and III collagen gene transcription in human skin fibroblasts. *J. Dermatol. Sci.* **1996**, *11* (3), 250-253. https://doi.org/10.1016/0923-1811(95)00640-0

(6) Desneves, K. J.; Todorovic, B. E.; Cassar, A.; Crowe, T. C. Treatment with supplementary arginine, vitamin C and zinc in patients with pressure ulcers: A randomised controlled trial. *Clin. Nutr.* **2005**, *24* (6), 979-987. https://doi.org/10.1016/j.clnu.2005.06.011

(7) Bechthold, A. New reference values for Vitamin C intake. *Ann. Nutr. Metab*. **2015**, *67* (1), 13-20. https://doi.org/10.1159/000434757

(8) Ogiri, Y.; Sun, F.; Hayami, S.; Fujimura, A.; Yamamoto, K.; Yaita, M.; Kojo, S. Very low vitamin C activity of orally administered L-dehydroascorbic acid. *J. Agric. Food Chem.* **2002**, *50*, 227-229. https://doi.org/10.1021/jf010910f

(9) Zhang, S. Q.; Wen, J.; Li, H. Y.; Chen, M. L. Iron modified hydrogen-bonded organic framework as fluorescent sensor for ascorbic acid detection. *Spectrochim. Acta, Part A* **2024**, *317*, 124393. https://doi.org/10.1016/j.saa.2024.124393
(10) Lu, X. C.; Wang, Z.; Wang, J. X.; Li, Y.; Hou, X. Q. Ultrasensitive Fluorescence Detection of Ascorbic Acid Using Silver Ion-Modulated High-Quality CdSe/CdS/ZnS Quantum Dots. *ACS Omega.* **2024**, *9* (25), 27127-27136. https://doi.org/10.1021/acsomega.4c01045
(11) Legrand, P.; Gahoual, R.; Benattar, R.; Toussaint, B.; Roques, C.; Mignet, N.; Goulay-Dufaÿ, S.; Houzé, P. Comprehensive and quantitative stability study of ascorbic acid using capillary zone electrophoresis with ultraviolet detection and high-resolution tandem mass spectrometry. *J. Sep. Sci.* **2020**, *43* (14), 2925-2935. https://doi.org/10.1002/jssc.202000389
(12) Sil, B. K.; Jamiruddin, M. R.; Haq, M. A.; Aekwattanaphol, N.; Ananth, K. P.; Salendra, L.; Paliwal, H.; Paul, P. K.; Buatong, W.; Srichana, T. Nanolevel of detection of ascorbic acid using horse-radish peroxidase inhibition assay. *Helioyn* **2024**, *10* (10), e30715. https://doi.org/10.1016/j.heliyon.2024.e30715
(13) Hasan, M. M.; Abu Reza, M.; Haque, A. Detection and Quantification of Ascorbic Acid in Citrus macroptera Fruit Pulp Juice by High Performance Liquid Chromatography. *Anal. Chem. Lett.* **2021**, *11* (2), 284-288. https://doi.org/10.1080/22297928.2021.1908911
(14) Huang, D.; Li, X.; Chen, M.; Chen, F.; Wan, Z.; Rui, R.; Wang R.; Fan S.; Wu, H. An electrochemical sensor based on a porphyrin dye-functionalized multi-walled carbon nanotubes hybrid for the sensitive determination of ascorbic acid. *J. Electroanal. Chem*. **2019**, *841*, 101-106. https://doi.org/10.1016/j.jelechem.2019.04.041
(15) Mohammadnezhad, K.; Ahour, F.; Keshipour, S. Electrochemical determination of ascorbic acid using palladium supported on N-doped graphene quantum dot modified electrode. *Sci. Rep.* **2024**, *14*, 5982. https://doi.org/10.1038/s41598-024-56231-x
(16) Li, N.; Nan, C.; Mei X.; Sun, Y.; Feng H.; Li Y. Electrochemical sensor based on dual-template molecularly imprinted polymer and nanoporous gold leaf modified electrode for simultaneous determination of dopamine and uric acid. *Microchim. Acta* **2020**, *187*, 496. https://doi.org/10.1007/s00604-020-04413-5
(17) Gutiérrez, A.; Ramírez-Ledesma, M. G.; Rivas, G. A.; Luna-Bárcenas, G.; Escalona-Villalpando, R. A.; Ledesma-García, J. Development of an electrochemical sensor for the quantification of ascorbic acid and acetaminophen in pharmaceutical samples. *J. Pharm. Biomed. Anal.* **2024**, *249*, 116334. https://doi.org/10.1016/j.jpba.2024.116334
(18) Silva Junior, G. J.; Selva, J. S. G.; Sukeri, S.; Gonçalves, J. M.; Regiart, M.; Bertotti, M. Fabrication of dendritic nanoporous gold via a two-step amperometric approach: Application for electrochemical detection of methyl parathion in river water samples. *Talanta* **2021**, *226*, 122130. https://doi.org/10.1016/j.talanta.2021.122130
(19) Chu, Y.; Zhou, H.; Wang, X.; Zhang, H.; Zhao, L.; Xu, T.; Yan, H.; Zhao, F. A flexible and self-supported nanoporous gold wire electrode with a seamless structure for electrochemical ascorbic acid sensor. *Microchem. J.* **2023**, *186*, 108259. https://doi.org/10.1016/j.microc.2022.108259
(20) Silva, T. A.; Khan, M. R. K.; Fatibello-Filho, O.; Collinson, M. Simultaneous electrochemical sensing of ascorbic acid and uric acid under biofouling conditions using nanoporous gold electrodes. *J. Electroanal. Chem*. **2019**, *846*, 113160. https://doi.org/10.1016/j.jelechem.2019.05.042
(21) Lins, R. S. O.; Sukeri, A.; Bertotti, M. A home-made nanoporous gold microsensor for lead(ii) detection in seawater with high sensitivity and anti-interference properties. *Anal. Methods* **2024**, *16*, 4415-4420. https://doi.org/10.1039/D4AY00698D
(22) Sakthivel, P.; Ramachandran, K.; Maheshvaran, K.; Senthil, T. S.; Manivel, P. Simultaneous electrochemical detection of ascorbic acid, dopamine and uric acid using Au decorated carbon nanofibers modified screen printed electrode. *Carbon Lett*. **2024**, *34* (9), 2325-2341. https://doi.org/10.1007/s42823-024-00759-5

(23) Kumar, A.; Furtado, V. L.; Gonçalves, J. M.; Bannitz-Fernandes, R.; Netto, L. E. S.; Araki, K.; Bertotti, M. Amperometric microsensor based on nanoporous gold for ascorbic acid detection in highly acidic biological extracts. *Anal. Chim. Acta* **2020**, *1095*, 61-70. https://doi.org/10.1016/j.aca.2019.10.022
(24) Paixão, T. R. L. C.; Lowinsohn, D.; Bertotti, M. Use of an Electrochemically Etched Platinum Microelectrode forAscorbic Acid Mapping in Oranges. *J. Agric. Food Chem*. **2006**, *54*, 3072-3077. https://doi.org/10.1021/jf052874g
(25) Kumar, A.; Gonçalves, J. M.; Furtado, V. L.; Araki, K.; Angnes, L.; Bouvet, M.; Meunier-Prest, R. Mass Transport in Nanoporous Gold and Correlation with Surface Pores for EC 1 Mechanism: Case of Ascorbic Acid. *ChemElectroChem* **2021**, *8* (11), 2129–2136. https://doi.org/10.1002/celc.202100440
(26) Bertotti, M.; Vaz, J. M.; Telles, R. Ascorbic Acid Determination in Natural Orange Juice: As a Teaching Tool of Coulometry and Polarography. *J. Chem. Educ.* **1995**, *72*, 445-447. https://doi.org/10.1021/ed072p445
(27) Veselinovic, J.; AlMashtoub, S.; Nagella, S.; Seker, E. Interplay of Effective Surface Area, Mass Transport, and Electrochemical Features in Nanoporous Nucleic Acid Sensors. *Anal. Chem.* **2020**, *92* (15), 10751-10758. https://doi.org/10.1021/acs.analchem.0c02104
(28) Mohd Zaki, M. H.; Mohd, Y.; Chin, L. Y. Surface Properties of Nanostructured Gold Coatings Electrodeposited at Different Potentials. *Int. J. Electrochem. Sci.* **2020**, *15* (11), 11401–11415. https://doi.org/10.20964/2020.11.41
(29) Sakthivel, P.; Ramachandran, K.; Maheshvaran, K.; Senthil, T. S.; Manivel, P. Simultaneous Electrochemical Detection of Ascorbic Acid, Dopamine and Uric Acid Using Au Decorated Carbon Nanofibers Modified Screen Printed Electrode. *Carbon Lett.* **2024**, *34* (9), 2325–2341. https://doi.org/10.1007/s42823-024-00759-5
(30) Currie, L. A. Nomenclature in Evaluation of Analytical Methods including Detection and Quantification Capabilities. *Anal. Chim. Acta* **1999**, *391*, 105-126. https://doi.org/10.1016/S0003-2670(99)00104-X
(31) Wei, Y.; Liu, Y.; Xu, Z.; Wang, S.; Chen, B.; Zhang, D.; Fang, Y. Simultaneous Detection of Ascorbic Acid, Dopamine, and Uric Acid Using a Novel Electrochemical Sensor Based on Palladium Nanoparticles/Reduced Graphene Oxide Nanocomposite. *Int. J. Anal. Chem*. **2020**, *2020*, 8812443. https://doi.org/10.1155/2020/8812443
(32) Silva, T. A.; Khan, M. R. K.; Fatibello-Filho, O.; Collinson, M. M. Simultaneous Electrochemical Sensing of Ascorbic Acid and Uric Acid under Biofouling Conditions Using Nanoporous Gold Electrodes. *J. Electroanal. Chem*. **2019**, *846*, 113160. https://doi.org/10.1016/j.jelechem.2019.05.042
(33) Cao, F.; Zhang, L.; Tian, Y. A Novel N-Doped Carbon Nanotube Fiber for Selective and Reliable Electrochemical Determination of Ascorbic Acid in Rat Brain Microdialysates. *J. Electroanal. Chem*. **2016**, *781*, 278–283. https://doi.org/10.1016/j.jelechem.2016.10.027
(34) Mazzara, F.; Patella, B.; Aiello, G.; O'Riordan, A.; Torino, C.; Vilasi, A.; Inguanta, R. Electrochemical Detection of Uric Acid and Ascorbic Acid Using r-GO/NPs Based Sensors. *Electrochim. Acta* **2021**, *388*, 138652. https://doi.org/10.1016/j.electacta.2021.138652
(35) Chu, W.; Zhou, Q.; Li, S.; Zhao, W.; Li, N.; Zheng, J. Oxidation and Sensing of Ascorbic Acid and Dopamine on Self-Assembled Gold Nanoparticles Incorporated within Polyaniline Film. *Appl. Surf. Sci*. **2015**, *353*, 425–432. https://doi.org/10.1016/j.apsusc.2015.06.141
(36) Pal, P.; Bhattacharjee, S.; Das, M. P.; Shim, Y.-B.; Neppolian, B.; Cho, B. J.; Veluswamy, P.; Das, J. Design of Electrochemically Reduced Graphene Oxide/Titanium Disulfide Nanocomposite Sensor for Selective Determination of Ascorbic Acid. *ACS Appl. Nano Mater*. **2021**, *4* (10), 10077–10089. https://doi.org/10.1021/acsanm.1c01464
(37) Krishnan, S.; Tong, L.; Liu, S.; Xing, R. A Mesoporous Silver-Doped TiO_2–SnO_2 Nanocomposite on g-C_3N_4 Nanosheets and Decorated with a Hierarchical Core−Shell Metal–Organic Framework for Simultaneous Voltammetric Determina-tion of Ascorbic Acid, Dopamine and Uric Acid. *Microchim. Acta* **2020**, *187* (1), 82. https://doi.org/10.1007/s00604-019-4045-x
(38) Robards, K.; Antolovich, M. Methods for Assessing the Authenticity of Orange Juice. A review. *The Analyst* **1995**, *120*, 1-28. https://doi.org/10.1039/an9952000001

(39) Battistuzzi, G.; D'Onofrio, M.; Loschi, L.; Sola, M. Isolation and Characterization of Two Peroxidases from *Cucumis sativus*. *Arch. Biochem. Biophys.* **2001**, *388*, 100-112. https://doi.org/10.1006/abbi.2001.2281

SUPPLEMENTARY MATERIAL

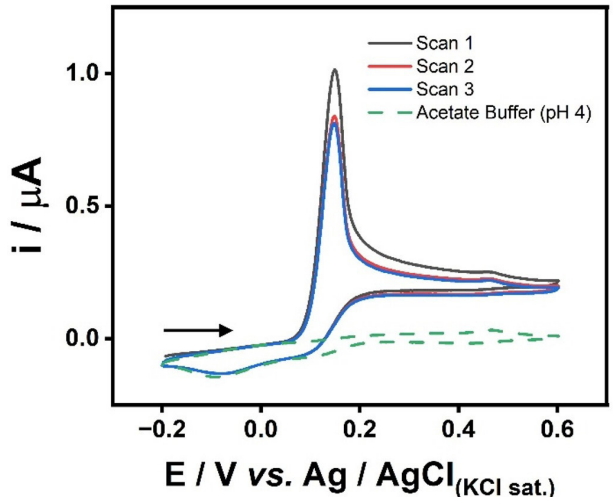

Figure 1S. Different CV cycles recorded in a 3.0 mmol L^{-1} AA in acetate buffer (pH 4.0) solution (black, red and blue curve) and a CV recorded in acetate buffer (pH 4.0) solution (green curve) using an NPG-modified electrode. Scan rate: 100 mV s^{-1}.

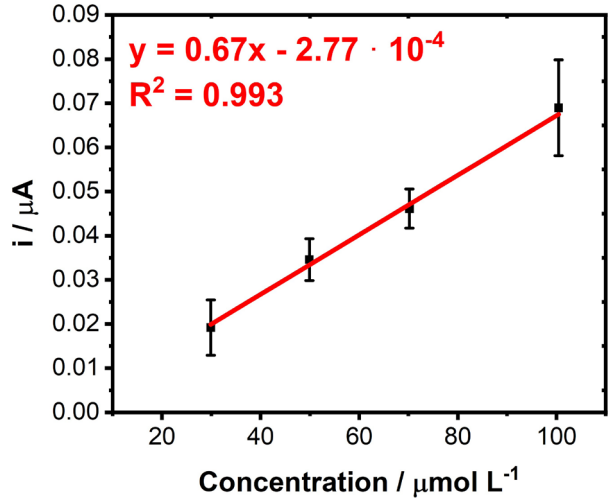

Figure 2S. Analytical curve between AA 30 and 100 μmol L^{-1} recorded in acetate buffer (pH 4.0) solutions using the NPG-modified electrode.

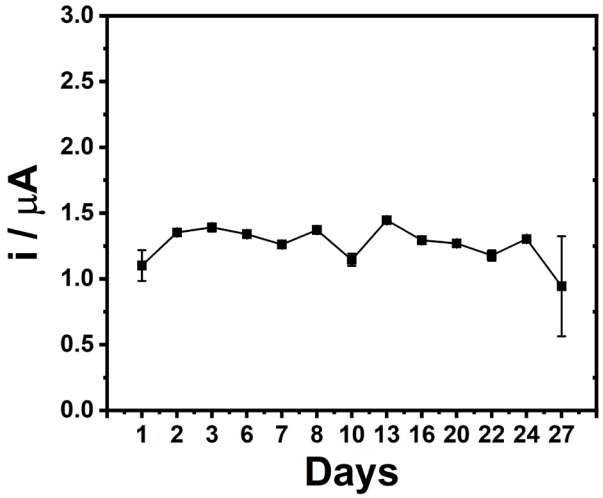

Figure 3S. Stability study results. Current was obtained by inserting the same NPG- modified electrode into a 3.0 mmol L^{-1} AA solution in acetate buffer (pH 4.0).

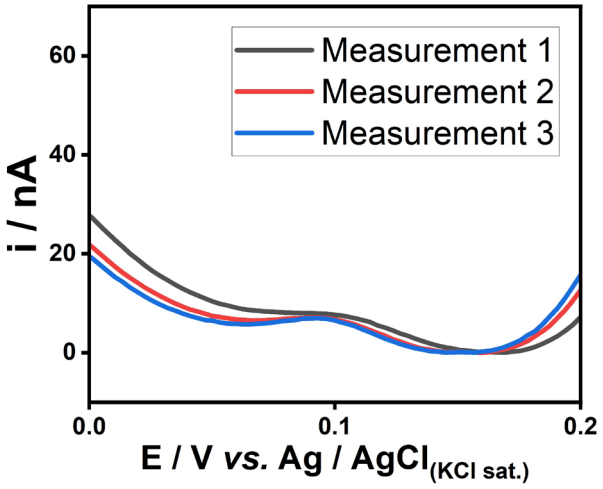

Figure 4S. Consecutive DPVs recorded in acetate buffer (pH 4) solution using an NPG-modified electrode. Between measurements, the sensor was kept in a solution containing AA to examine the memory effect.